VYSOKÉ UČENÍ TECHNICKÉ V BRNĚ
BRNO UNIVERSITY OF TECHNOLOGY

FAKULTA INFORMAČNÍCH TECHNOLOGIÍ
ÚSTAV POČÍTAČOVÉ GRAFIKY A MULTIMÉDIÍ

FACULTY OF INFORMATION TECHNOLOGY
DEPARTMENT OF COMPUTER GRAPHICS AND MULTIMEDIA

AUTOMATIC FLIGHT CONTROL SYSTEM DESIGN FOR A JET AIRCRAFT

BAKALÁŘSKÁ PRÁCE
BACHELOR'S THESIS

AUTOR PRÁCE
AUTHOR

MILAN KRASŇANSKÝ

BRNO 2015

VYSOKÉ UČENÍ TECHNICKÉ V BRNĚ
BRNO UNIVERSITY OF TECHNOLOGY

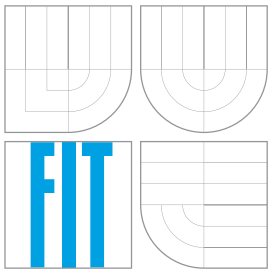

FAKULTA INFORMAČNÍCH TECHNOLOGIÍ
ÚSTAV POČÍTAČOVÉ GRAFIKY A MULTIMÉDIÍ

FACULTY OF INFORMATION TECHNOLOGY
DEPARTMENT OF COMPUTER GRAPHICS AND MULTIMEDIA

NÁVRH AUTOMATICKÉHO SYSTÉMU ŘÍZENÍ LETU PRO PROUDOVÝ LETOUN

AUTOMATIC FLIGHT CONTROL SYSTEM DESIGN FOR A JET AIRCRAFT

BAKALÁŘSKÁ PRÁCE
BACHELOR'S THESIS

AUTOR PRÁCE — MILAN KRASŇANSKÝ
AUTHOR

VEDOUCÍ PRÁCE — Ing. PETER CHUDÝ, Ph.D., MBA
SUPERVISOR

BRNO 2015

Abstrakt

Tato bakalářská práce se zabývá modelováním letových vlastností proudového letadla a následným návrhem a implementací systému pro automatické řízení letu. Jejím cílem bylo na základě veřejně dostupných aerodynamických dat letounu F-16, který má sníženou podélnou stabilitu, implementovat model tohoto letounu a použít tento model jako platformu pro návrh a implementaci systému pro automatické řízení letu založeného na nelineární dynamické inverzi se soustředením se na řízení podélného pohybu letounu, pomocí nastavení požadovaného úhlu náběhu. Testy vytvořeného systému prokázali schopnost dosáhnout a udržet požadovaný úhel náběhu.

Abstract

This bachelor's thesis deals with the modelling of flight characteristics of a jet airplane and subsequent design and implementation of an automatic flight control system. Its goal was to implement a model of a jet airplane based on publicly available aerodynamic data of F-16 aircraft and use this model as a platform for the design and implementation of an automatic flight control system based on the non-linear dynamic inversion with a focus on controlling the pitch angle of an airplane by setting a desired value of the angle of attack. Conducted tests of the created system proved the ability of the control system to reach and maintain the desired angle of attack.

Klíčová slova

matematický model letounu, systém řízení letu, autopilot, nelineární dynamická inverze

Keywords

mathematical model of an airplane, flight control system, autopilot, non-linear dynamic inversion

Citace

Milan Krasňanský: Automatic Flight Control System Design for a Jet Aircraft, bakalářská práce, Brno, FIT VUT v Brně, 2015

Automatic Flight Control System Design for a Jet Aircraft

Prohlášení

Prohlašuji, že jsem tuto bakalářskou práci vypracoval samostatně pod odborným vedením pana Ing. Petra Chudého, PhD. MBA

.....
Milan Krasňanský
May 18, 2015

Poděkování

Rád bych poděkoval Ing. Petrovi Chudému, PhD. MBA za jeho příkladné vedení, trpělivost, cenné rady a množství času, který mi při tvorbě tohoto díla věnoval. Dále bych chtěl poděkovat celé skupině Aeroworks, díky které jsem měl příležitost vidět jak vypadá výzkum v oblasti letectva.

Contents

List of Figures

List of Tables

List of symbols

a	semi-major axis m
a_n	normal acceleration, positive along negative Z body axis, g units
a_y	lateral acceleration, positive along positive Y body axis
b	wing span, m
c	speed of sound, $m.s^{-1}$
C_L	lift coefficient
C_l	rolling-moment coefficient about X body axis
$C_{l,t}$	total rolling-moment coefficient
C_m	pitching-moment coefficient about Y body axis
$C_{m,t}$	total pitching-moment coefficient
C_n	yawing-moment coefficient about Z body axis
$C_{n,t}$	total yawing-moment coefficient
C_n	X-axis force coefficient along positive X body axis
$C_{X,t}$	total X-axis force coefficient
C_Y	Y-axis force coefficient along positive Y body axis
$C_{Y,t}$	total Y-axis force coefficient
C_Z	Z-axis force coefficient along positive Z body axis
$C_{Z,t}$	total Z-axis force coefficient
$\overline{c}$	wing mean aerodynamic chord, m

e	first eccentricity, [1]
f	flattening, [1]
F_{lat}	pilot lateral stick force, positive for right roll, N
F_{long}	pilot longitudinal stick force, positive for aft force, N
F_{ped}	pilot pedal force, positive for right yaw, N
g	acceleration due to gravity, $m.sec^{-2}$
H_e	engine angular momentum, $kg.m^{-2}.sec^{-1}$
h	altitude, m
I_X, I_Y, I_Z	moments of inertia about X,Y and Z body axes, $kg.m^{-2}$
I_{XZ}	product of inertia with respect to X and Z body axes, $kg.m^{-2}$
K_i	integral gain, [1]
K_p	proportional gain, [1]
M	Mach number, [1]
M_μ	meridian radius of curvature, [1]
m	airplane mass, kg
N_μ	prime vertical radius of curvature, [1]
P_1	engine power command based on throttle position, percent of maximum power
P_1	engine power command to engine, percent of maximum power
P_3	engine power, percent of maximum power
p	airplane roll rate about X body axis, $rad.sec^{-1}$
P_s	static pressure, $N.m^{-2}$
q	airplane pitch rate about Y body axis, $rad.sec^{-1}$
q_c	commanded airplane pitch rate about Y body axis, $rad.sec^{-1}$
q_{RM}	airplane pitch rate about Y body axis from reference model, $rad.sec^{-1}$

$\dot{q}$	airplane pitch acceleration about Y body axis, $rad.sec^{-1}$
$\overline{q}$	free-stream dynamic pressure, $N.m^{-2}$
r	yaw rate about Z body axis, $rad.sec^{-1}$
r_f	filtered yaw-rate signal, $rad.sec^{-1}$
$\dot{r}$	yaw acceleration about Z body axis, $rad.sec^{-2}$
S	wing area, m^2
T	total instantaneous engine thrust, N
T_{idle}	idle thrust, N
T_{max}	maximum thrust, N
T_{mil}	military thrust, N
T_K	temperature, K
T_s	reference model gain,
t	time, s
u, v, w	components of airplane velocity along X,Y and Z body axes, $m.sec^{-1}$
V	airplane resultant velocity, $m.sec^{-1}$
$\dot{w}$	airplane acceleration along Z body axis, $m.sec^{-2}$
X, Y, Z	airplane body axes
X_{cg}	center-of-gravity location, fraction of $\overline{c}$, [1]
$X_{cg,ref}$	reference center-of-gravity location for aerodynamic data, [1]
α	angle of attack, deg
α_c	commanded angle of attack, deg
α_f	filtered angle-of-attack signal, deg
α_i	indicated angle of attack, deg
α_{RM}	angle of attack from reference model, deg

β	angle of sideslip, deg
δ_a	aileron deflection, positive for left roll, deg
$\delta_{a,c}$	aileron deflection commanded by control system, deg
δ_h	horizontal stabilator deflection, positive fro airplane nose-down control, deg
$\delta_{h,c}$	horizontal stabilator deflection commanded by control system, deg
δ_{lef}	leading-edge flap deflection, positive for leading edge flap down, deg
δ_r	rudder deflection, positive for left yaw, deg
δ_{sb}	speed-brake deflection, deg
$\dot{\gamma}$	virtual control input, [1]
η	horizontal stabilator effectiveness factor, [1]
θ, ϕ, ψ	euler angles , deg
τ	engine-thrust time constant, s

1. Introduction

Since the first flight of the Wright Flyer back in 1903, airplanes, as well as other flying vehicles, have been an important part of our society, even though they were first seen as a hobby of a few enthusiasts. People quickly realized their potential and started using them for all thinkable purposes, which led to rapid development of aircrafts. Nowadays, aircrafts provide convenient and fast mean of transport for both passengers and cargo, and are also used in sport, research or serve in armed forces.

A conventional aircraft is controlled by pilot, who uses a yoke or a joystick and pedals to control the deflection of aircraft's control surfaces. Historically, the yoke or the joystick was mechanically connected to the corresponding control surface using cables and rods and possibly hydraulic system (used mainly in heavier and more powerful aicraft), when pilot's muscle power alone may not be sufficient to provide enough strength do deflect the aircraft's control surfaces.

In 1960's, with the development of the spacecraft and airplanes with relaxed stability to favor better maneuverability, a need for a better control system emerged, resulting in the development of a fly-by-wire flight control system, which replaces the mechanical connections with electrical wires. These wires are used to transmit an electrical signal from pilot's inceptors to the actuators at each control surface. A alight control computer may also be engaged in the process, determining how to move corresponding actuators.

The first aircraft ever, which had a digital fly-by-wire with no mechanical backup, was the Lunar Landing Research Vehicle [11] used to simulate the Moon landing in Apollo program. This was followed by an experimental fly-by-wire version of the F-8 Crusader airplane and experimental fly-by-wire equipped Hawker Hunter [31] in the USA and Great Britain, respectively. Since then, fly-by-wire became a standard in modern aircraft and is widely used in civilian airliners, military airplanes and recently found it's way into helicopters [27].

The advantages of such flight control system are in the weight reduction, convenient backup options, the ability to filter pilot's input and thus preventing aircraft from exceeding standard flight envelope, the possibility of a fully automated flight or enhancing performance of an aircraft, all of which improve flight safety and reduce flight crew workload [31].

This document is divided into several chapters. The first part of the chapter 2 discusses the configuration of the conventional airplane and the description of an airplane used in simulation, while the second part focuses on modelling particular airplane dynamics including the equations of motions, moments, aerodynamic coefficients and other necessary equations used in simulation. Chapter 3 deals with the non-linear flight control systems used in modern control theory, while chapter 4 discusses the flight control systems implemented in this thesis. The examples of the results obtained during simulation runs with the implemented flight control system are presented in chapter 5. Possible future development or improvements to this thesis are discussed in chapter 6. Thesis ends with concluding remarks in chapter 7. Appendices contain the logic diagram of the thrust system in appendix

A, derivatives of aerodynamic coefficients in appendix B and the content of the enclosed DVD disc in appendix C.

2. Airplane Dynamic Model

As this thesis deals with design and implementation of a flight control system for an airplane, it is necessary to implement a simulation model of the airplane. At first, we should define what airplane is, what are its main parts and how it is controlled in the air. The section 2.1 of this chapter acquaints the reader with the configuration of a conventional airplane, while the second section 2.2 presents description of F-16 aircraft, which has been chosen to be modelled in this thesis.

2.1 Airplane

An airplane is a powered fixed-wing aicraft equipped with an engine (thus propelled by a propeller or a jet engine). The airplane has proved to be the most economical type of aircraft in terms of force needed to overcome aerodynamic drag, because the airplane has the best ratio of lift force and drag among all powered aircrafts. A disadvantage of an airplane is its inability to maintain altitude (in other words: stay in the air) without any forward speed (or when forward speed is below minimum), because wings and fuselage would not generate enough lift force. This implies significant risk of crash in case of a failure of the engine and the consequence is that the airplane can not stop in the air in case of encountering an obstacle and also needs a runway of significant length for take-off and landing (needed length depends on a particular airplane type). This disadvantage is reduced either by using multiple engines (and thus reducing the possibility of losing all the power) or/and ability to glide for a limited period of time [25]. The airplane consists of three main components [18]:

1. Airframe
2. Propulsion systems
3. Avionics systems

2.1.1 Airframe

Airframe is the mechanical structure of the airplane [18]. Airframe generates lift, which is necessary to enable the airplane to fly and also provides the space for the crew, passengers, cargo, fuel and avionics. An airframe consists of several parts:

Wings Wings are part of the airframe, which create the biggest percentage of aerodynamic lift force and, in conventional airplane, are symmetrical on both port and starboard sides of the airplane. Wing has an aerofoil shape [18]. As the aerofoil-shaped object (e.g. wing) passes through fluid, it deflects air (in other words, it applies force on the air), which

Figure 2.1: An airplane. British Aerospace Hawk T1 of the Royal Air Force Aerobatic Team, the Red Arrows

results in force on aerofoil in opposite direction [15]. Another feature of the wing is the sweep angle which varies: airplane may have straight wings, swept wings, forward-swept wings or variable geometry of the wing [18]. Wings also serve as a bearer of the control surfaces, namely the aileron, flaps, spoilers and their potential combinations and, of course, either mechanical or electronic connections between the control surfaces and the cockpit. It is also not uncommon to use the available space in wings to house additional internal fuel tanks [25].

Fuselage A fuselage connects all other parts of the airframe and also provides the space for the crew, passengers and cargo. An engine is also frequently located in the fuselage. The fuselage is the main source of the aerodynamic drag of the airplane. However the fuselage also generates lift force, which is usually much smaller than the lift force generated by wings [18]. Although some airplanes, such as Mikoyan-Gurevich MiG-29, may have up to 40 % of total lift force generated by the fuselage [10].

Horizontal (tailplane) and vertical (fin) stabilizer The horizontal stabilizer is usually mounted on the rear of the fuselage. Its purpose is to stabilize the airplane along its pitch axis. Fin is a wing-like surface mounted vertically on the rear of the fusalage with the purpose of to stabilize the airplane along its yaw axis [18].

Landing gear A landing gear, either retractable or fixed, is a device which enables the aircraft to land, take off and taxi on the ground using wheels, on the water using floats or on the snow using landing skis [18]. It absorbs kinetic energy of an airplane during landing. As the landing gear has no fuction during the actual flight as it adds weight, there is usually effort to minimize the weight of the landing gear.

Control surfaces Control surfaces are the means of how to control the airplane in the air. By changing the deflection of the control surfaces, the pilot or the flight computer can manoeuvre the airplane in the air. Three main flight control surfaces are the ailerons, which

are mounted on the wings and their deflection rotate the airplane along its longitudinal (roll) axis. The elevator, which is usually mounted on the horizontal stabilizer and its deflection rotates the airplane along lateral (pitch) axis, and a rudder, which is usually mounted on the vertical stabilizer and rotates the airplane along vertical (yaw) axis. Other control surfaces include canards, tailerons, flaperons, trailing-edge flaps, leading-edge flaps and more [18].

2.1.2 Propulsion

The propulsion system generates thrust. When engine accelerates the aircraft in one direction a reaction force will be of the same magnitude but the opposite direction according to Newton's laws [21]. This reaction force is called thrust and is used to accelerate the airplane to a speed, when the aiframe generates enough aerodynamic lift force to lift the airplane up in the air. Fixed-wing airplanes use piston, turboprop, jet or rocket engines to accomplish that [18].

2.1.3 Avionics

Avionics are electronics system (aviation electronics) used in an airplane. The avionics include all communication and navigation system as well as radar, flight control systems, ejection seats and other electrical instruments [25].

2.2 General Dynamics F-16 Fighting Falcon

An airplane which is used as a basis for the flight control is a General Dynamics F-16 Fighting Falcon. The F-16 has been chosen due to the public availiability of its aerodynamic data from NASA [22].

Figure 2.2: F-16AM MLU of the Royal Netherlands Air Force Demo Team

2.2.1 Basic description

A General Dynamics (later Lockheed Martin) F-16 Fighting Falcon is a single- or two-seat single-engine supersonic multi-role combat aircraft designed in the late 1960s and early

1970s in the United States of America. Since then, it has become one of the most famous and most succesful fighter aircraft in the world with more than 25 operators worldwide and more than 4500 aircrafts produced [6]. An F-16 design used many technologies, which were back then considered „state-of-the-art“ such as variable camber wing, vortex lift, blended wing-body, console-mounted stick, relaxed longitudal stability and fly-by-wire [7].

2.2.2 Aerodynamic characteristics

As mentioned earlier, an F-16 features a so called relaxed longitudinal stability concept, which means that the airplane has been deliberately designed to be aerodynamically unstable in pitch axis to enhance maneuverability. In other words, an F-16 tends to pitch up [16]. This feature helps the maneuverability of the airplane but necessitates a flight control system [11]. Therefore, the F-16 features onboard quadruple-redundant fly-by-wire [16] and was one of the first two U.S. Air Force airplanes to feature fly-by-wire (the other one being the F/A-18) [20].

2.2.3 F-16 Control Surfaces

An airplane configuration of an F-16 is shown in figure 2.3. The primary aerodynamic controls include a symmetrical deflection of a horizontal stabilator for the pitch control, a deflection of conventional wing-mounted flaperons (flaps combined with ailerons) and a differential deflection of the horizontal stabilators for the roll control and the rudder deflection for the yaw control. Another control surfaces of the F-16 are flaps mounted on the leading-edge of the wing and the speedbrakes mounted on the fuselage on both sides of the engine nozzle.

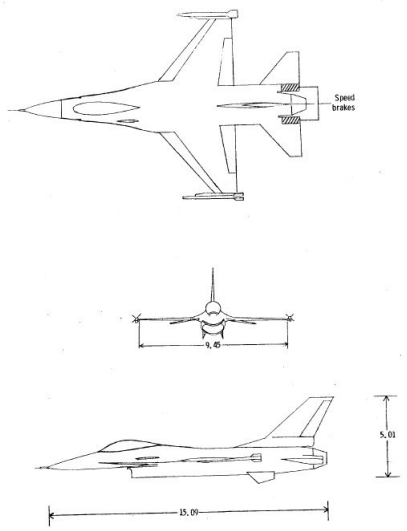

Figure 2.3: F-16 three-view drawing. All dimensions are given in meteres [22]

2.3 Modelling the Airplane

The essential part of designing and developing a control system is the modelling if the system, which is intended to be controlled. As this thesis deals with implementation of the

flight control system for an airplane, an airplane and especially its dynamic characteristics needs to be modelled. The description of the airplane used in the simulation can be found in section 2.2.

For creating the model (and also for the subsequent creating the flight control system) a *Matlab Simulink* software has been chosen, as they represent an industry grade rapid prototyping tool for such applications.

2.4 Model Limitations

It should be noted that only the flight characteristics of the F-16 were modelled in this thesis. The utilized model does not contain the characteristics of the groundmotion (taxiing) and also does not provide the option to simulate landing or take-off. Due to the lack of the aerodynamic data, following features of a real-world airplane were not modelled: differential deflection of the horizontal stabilator, deflection of the speed brake, deflection of the trailing-edge flaps and flight with an extended landing gear. Moreover, aerodynamic data (and therefore the model itself) are valid only for speed up to Mach 0.6 [22].

2.5 Assumptions

- The airplane is a rigid body. A rigid body is ideal solid body in which the deformation is neglected. In other words, regardless of external forces, a distance between two given points remains constant. This assumption is valid for an airplane of the F-16's category [27].
- Wind is assumed to be at rest with respect to the surface of the Earth.
- The airplane is in clean configuration (no ordnance or external fuel tanks).
- The airplane has a constant mass.
- The air is assumed to be incompressible.

2.6 Equations of Motions

All equations are non-linear, six-degree-of-freedom equations referenced to a body-fixed reference frame shown in figure 2.4. Equations of aerodynamic coefficients $C_{x,t}$, $C_{y,t}$, $C_{z,t}$, $C_{l,t}$, $C_{m,t}$, $C_{n,t}$, equations of Euler angles and other auxiliary equations are defined in following sections. Value of T (thrust) is computed according to the logic diagram shown in figure A.1. Value of the airplane constants used in equations of motions can be found in table 2.1.The gravitational acceleration was modelled as a constant value of $9.80665\,ms^{-2}$ [1].

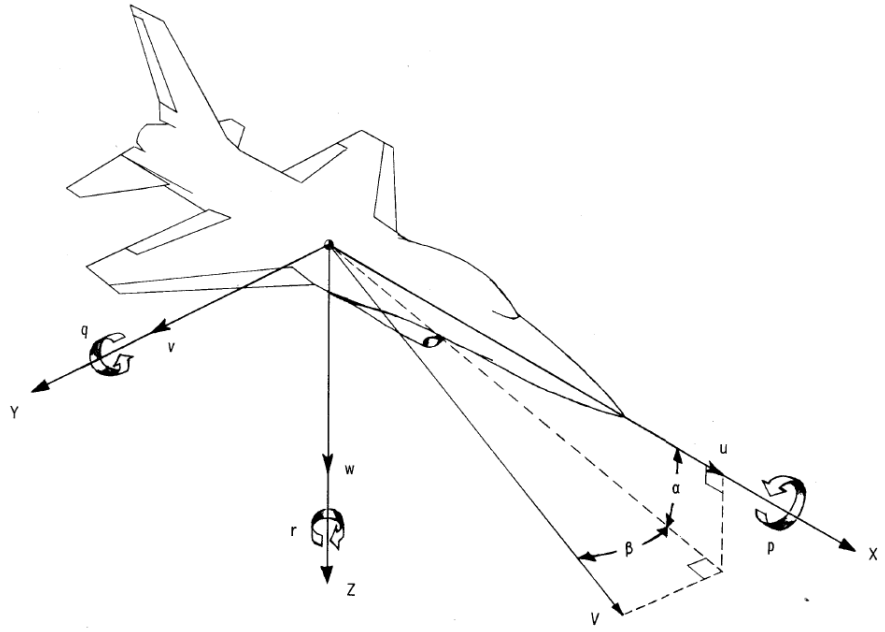

Figure 2.4: Body system of axes [22]

2.6.1 Forces

The forces are components of airplane velocity along its axis shown in figure 2.4. The unit is meters per second ($m.s^{-1}$).

$$\dot{u} = rv - qw - g\sin\theta + \frac{\bar{q}S}{m}C_{x,t} + \frac{T}{m} \tag{2.1}$$

$$\dot{v} = pw - ru - g\cos\theta\sin\phi + \frac{\bar{q}S}{m}C_{y,t} \tag{2.2}$$

$$\dot{w} = qu - pv - g\cos\theta\cos\phi + \frac{\bar{q}S}{m}C_{z,t} \tag{2.3}$$

2.6.2 Moments

Moments are airplane rates along its axis. The unit is radians per second ($rad.s^{-1}$).

$$\dot{p} = \frac{I_Y - I_Z}{I_X}qr + \frac{I_{XZ}}{I_X}(\dot{r} + pq) + \frac{\bar{q}Sb}{I_X}C_{l,t} \tag{2.4}$$

$$\dot{q} = \frac{I_Z - I_X}{I_Y}pr + \frac{I_{XZ}}{I_Y}(r^2 - p^2) + \frac{\bar{q}S\bar{c}}{I_Y}C_{m,t} - \frac{H_e r}{I_Y} \tag{2.5}$$

$$\dot{r} = \frac{I_X - I_Y}{I_Z}pq + \frac{I_{XZ}}{I_Z}(\dot{p} - qr) + \frac{\bar{q}Sb}{I_Y}C_{n,t} + \frac{H_e q}{I_Z} \tag{2.6}$$

2.7 Aerodynamic Coefficients

Following equations define the aerodynamic coefficients used in equations of motions [22]. The aerodynamic coefficients are referenced to a center-of-gravity location of $0.35\bar{c}$. The aerodynamic data used in these equations consist of 64 tables of values, which were derived from static and dynamic wind-tunnel tests using an F-16 subscale models at NASA Ames and Langley Research Center. The values of aerodynamic data can be found in [22]. An example of the data is shown in figure 4.1.

X-axis force coefficient [22]:

$$C_{X,t} = C_X(\alpha,\beta,\delta_h) + \Delta C_{X,lef}\left(1-\frac{\delta_{lef}}{25}\right) + \Delta C_{X,sb}(\alpha)\left(\frac{\delta_{sb}}{60}\right) + \frac{\bar{c}v}{2V}\left[C_{X_q}(\alpha) + \Delta C_{X_{q,lef}}(\alpha)\left(1-\frac{\delta_{lef}}{25}\right)\right] \tag{2.7}$$

where

$$\Delta C_{X,lef} = C_{X,lef}(\alpha,\beta) - C_X(\alpha,\beta,\delta_h = 0^\circ)$$

Z-axis force coefficient [22]:

$$C_{Z,t} = C_Z(\alpha,\beta,\delta_h) + \Delta C_{Z,lef}\left(1-\frac{\delta_{lef}}{25}\right) + \Delta C_{Z,sb}(\alpha)\left(\frac{\delta_{sb}}{60}\right) + \frac{\bar{c}q}{2V}\left[C_{Z_q}(\alpha) + \Delta C_{Z_{q,lef}}(\alpha)\left(1-\frac{\delta_{lef}}{25}\right)\right] \tag{2.8}$$

where

$$\Delta C_{Z,lef} = C_{Z,lef}(\alpha,\beta) - C_Z(\alpha,\beta,\delta_h = 0^\circ)$$

Pitching-moment coefficient [22]:

$$\begin{aligned} C_{m,t} = {} & C_m(\alpha,\beta,\delta_h)\eta_{\delta_h}(\delta_h) + \Delta C_{Z,t}(X_{cg,ref} - X_{cg}) + \Delta C_{m,lef}\left(1-\frac{\delta_{lef}}{25}\right) \\ & + \Delta C_{m,sb}(\alpha)\left(\frac{\delta_{sb}}{60}\right) + \frac{\bar{c}q}{2V}\left[C_{m_q}(\alpha) + \Delta C_{m_{q,lef}}(\alpha)\left(1-\frac{\delta_{lef}}{25}\right)\right] \\ & + \Delta C_m(\alpha) + \Delta C_{m,ds}(\alpha,\delta_h) \end{aligned} \tag{2.9}$$

where

$$\Delta C_{m,lef} = C_{m,lef}(\alpha,\beta) - C_m(\alpha,\beta,\delta_h = 0^\circ)$$

Y-axis force coefficient [22]:

$$
\begin{aligned}
C_{Y,t} = {} & C_Y(\alpha,\beta) + \Delta C_{Y,lef}\left(1 - \frac{\delta_{lef}}{25}\right) \\
& + \left[\Delta C_{Y,\delta_{a=20^\circ}} + \Delta C_{Y\delta_{a=20^\circ},lef}\left(1 - \frac{\delta_{lef}}{25}\right)\right]\left(\frac{\delta_a}{20}\right) \\
& + \Delta C_{Y\delta_{r=30^\circ}}\left(\frac{\delta_r}{30}\right) + \frac{b}{2V}\left\{\left[C_{Y_r}(\alpha) + \Delta C_{Y_{r,lef}}(\alpha)\left(1 - \frac{\delta_{lef}}{25}\right)\right]r\right. \\
& \left. + \left[C_{Y_p}(\alpha) + \Delta C_{Y_{p,lef}}(\alpha)\left(1 - \frac{\delta_{lef}}{25}\right)\right]p\right\}
\end{aligned}
\tag{2.10}
$$

where

$$
\begin{aligned}
\Delta C_{Y,lef} &= C_{Y,lef}(\alpha,\beta) - C_Y(\alpha,\beta) \\
\Delta C_{Y,\delta_{a=20^\circ}} &= C_{Y,\delta_{a=20^\circ}} - C_Y(\alpha,\beta) \\
\Delta C_{Y,\delta_{a=20^\circ},lef} &= C_{Y,\delta_{a=20^\circ},lef} - C_{Y,lef}(\alpha,\beta) - \left[C_{Y,\delta_{a=20^\circ}} - C_Y(\alpha,\beta)\right] \\
\Delta C_{Y\delta_{r=30^\circ}} &= C_{Y\delta_{r=30^\circ}}(\alpha,\beta) - C_Y(\alpha,\beta)
\end{aligned}
$$

Yawing-moment coefficient [22]:

$$
\begin{aligned}
C_{n,t} = {} & C_n(\alpha,\beta,\delta_h) + \Delta C_{n,lef}\left(1 - \frac{\delta_{lef}}{25}\right) + C_{Y,t}(X_{cg,ref} - X_{cg})\frac{\overline{c}}{b} \\
& + \left[\Delta C_{n,\delta_{a=20^\circ}} + \Delta C_{n\delta_{a=20^\circ},lef}\left(1 - \frac{\delta_{lef}}{25}\right)\right]\left(\frac{\delta_a}{20}\right) \\
& + \Delta C_{n\delta_{r=30^\circ}}\left(\frac{\delta_r}{30}\right) + \frac{b}{2V}\left\{\left[C_{n_r}(\alpha) + \Delta C_{n_{r,lef}}(\alpha)\left(1 - \frac{\delta_{lef}}{25}\right)\right]r\right. \\
& \left. + \left[C_{n_p}(\alpha) + \Delta C_{n_{p,lef}}(\alpha)\left(1 - \frac{\delta_{lef}}{25}\right)\right]p\right\}
\end{aligned}
\tag{2.11}
$$

where

$$
\begin{aligned}
\Delta C_{n,lef} &= C_{n,lef}(\alpha,\beta) - C_n(\alpha,\beta,\delta_h^\circ) \\
\Delta C_{n,\delta_{a=20^\circ}} &= C_{n,\delta_{a=20^\circ}} - C_n(\alpha,\beta,\delta_h^\circ) \\
\Delta C_{n,\delta_{a=20^\circ},lef} &= C_{n,\delta_{a=20^\circ},lef} - C_{n,lef}(\alpha,\beta) - \left[C_{n,\delta_{a=20^\circ}} - C_n(\alpha,\beta,\delta_h^\circ)\right] \\
\Delta C_{n\delta_{r=30^\circ}} &= C_{n\delta_{r=30^\circ}}(\alpha,\beta) - C_n(\alpha,\beta,\delta_h^\circ)
\end{aligned}
$$

Rolling-moment coefficient:

$$
\begin{aligned}
C_{l,t} &= C_l(\alpha,\beta,\delta_h) + \Delta C_{l,lef}\left(1-\frac{\delta_{lef}}{25}\right) \\
&+ \left[\Delta C_{l,\delta_{a=20^\circ}} + \Delta C_{l\delta_{a=20^\circ},lef}\left(1-\frac{\delta_{lef}}{25}\right)\right]\left(\frac{\delta_a}{20}\right) \\
&+ \Delta C_{l\delta_{r=30^\circ}}\left(\frac{\delta_r}{30}\right) + \frac{b}{2V}\left\{\left[C_{l_r}(\alpha) + \Delta C_{l_r,lef}(\alpha)\left(1-\frac{\delta_{lef}}{25}\right)\right]r\right. \\
&+ \left.\left[C_{l_p}(\alpha) + \Delta C_{l_p,lef}(\alpha)\left(1-\frac{\delta_{lef}}{25}\right)\right]p\right\} + \Delta C_{l_\beta}(\alpha)\beta
\end{aligned}
\tag{2.12}
$$

where

$$
\begin{aligned}
\Delta C_{l,lef} &= C_{l,lef}(\alpha,\beta) - C_l(\alpha,\beta,\delta_h^\circ) \\
\Delta C_{l,\delta_{a=20^\circ}} &= C_{l,\delta_{a=20^\circ}} - C_l(\alpha,\beta,\delta_h^\circ) \\
\Delta C_{l,\delta_{a=20^\circ},lef} &= C_{l,\delta_{a=20^\circ},lef} - C_{l,lef}(\alpha,\beta) - \left[C_{l,\delta_{a=20^\circ}} - C_l(\alpha,\beta,\delta_h^\circ)\right] \\
\Delta C_{l\delta_{r=30^\circ}} &= C_{l\delta_{r=30^\circ}}(\alpha,\beta) - C_l(\alpha,\beta,\delta_h^\circ)
\end{aligned}
$$

2.8 Auxiliary equations

The auxiliary equations are used to compute the values of the variables in the equations of motions and equations of the aerodynamic coefficients as well as other variables needed in simulation. The equations are taken from [22] if not stated otherwise.

2.8.1 Angle of Attack and Angle of Sideslip

The Angle of Attack is the angle between the oncoming air (relative wind) and a reference line of the airplane [4]. In our case, the reference line is the x-axis (longitudinal) in body fixed system shown in figure 2.4.

Angle of sideslip is an angle between the x-axis (longitudinal) and velocity vector shown in figure 2.4.

$$\alpha = \arctan\left(\frac{w}{u}\right) \tag{2.13}$$

$$\beta = \arcsin\left(\frac{v}{V}\right) \tag{2.14}$$

2.8.2 Velocity and acceleration

The airplane velocity consists of three components (u, v, w) as shown in equation 2.15. The accelerations a_n and a_y are the normal and the lateral accelerations, respectively.

$$V = \sqrt{u^2 + v^2 + w^2} \tag{2.15}$$

$$a_n = \frac{qu - pv + g\cos\theta\cos\phi - \dot{w}}{g} \tag{2.16}$$

$$a_y = \frac{-pw + ru + g\cos\theta\sin\phi - \dot{v}}{g} \tag{2.17}$$

2.8.3 Dynamic pressure

As we assume the air is incompressible (2.5), it is possible to use following equation to compute the dynamic pressure [12]:

$$q = \frac{1}{2}\rho v^2 \tag{2.18}$$

where value of the air density (ρ) is computed from the static air pressure, temperature and altitude [13]. The equation of altitude is given in section 2.8.6.

$$\rho = \frac{P_s}{T_K + 287.058} \tag{2.19}$$

$$\tag{2.20}$$

where

$$T_K = \begin{cases} 216.65 & \text{for } 11000\,m \leq h \leq 20000\,m \\ 288.15 - 6.5 * (\frac{h}{1000}) & \text{for } 0\,m \leq h \leq 11000\,m \end{cases} \tag{2.21}$$

$$P_s = \begin{cases} 226.320^{1.7345737 - 1.5768852 * 10^{-4h}} & \text{for } 11000\,m \leq h \leq 20000\,m \\ (3.731444 - 0.841728 * 10^{-4h})^{5.255880} & \text{for } -1450\,m \leq h \leq 11000\,m \end{cases} \tag{2.22}$$

2.8.4 Speed of sound

As the available aerodynamic data are valid only for the speed up to Mach 0.6 [22], a saturation of the speed at this value has been added to the model in order not to reach the state, where the behaviour of the airplane is not defined by the available data. This is achieved by dynamic saturation using *Simulink* built-in block.

Following equation has been used to compute speed of sound [13]:

$$c = 20,046796\sqrt{T_K} \tag{2.23}$$

where T_K is temperature in Kelvin.

And maximum permissible speed is then defined as:

$$V_{max} = 0.6c \tag{2.24}$$

2.8.5 Euler Angles

Euler angles determine attitude of an airplane and were computed from the moments using following transformation matrix [29]:

$$\begin{bmatrix} \dot{\theta} \\ \dot{\phi} \\ \dot{\psi} \end{bmatrix} = \begin{bmatrix} 1 & \sin\phi\tan\theta & \cos\phi\tan\theta \\ 0 & \cos\phi & -\sin\phi \\ 0 & \frac{\sin\phi}{\cos\theta} & \frac{\cos\phi}{\cos\theta} \end{bmatrix} . \begin{bmatrix} p \\ q \\ r \end{bmatrix} \tag{2.25}$$

2.8.6 Position differential equation

To determine the airplane's position, coordinates (latitude, longitude and altitude) in geodetic coordinate system are computed [2]:

LLA coordinates:

$$\begin{bmatrix} \dot{\lambda} \\ \dot{\mu} \\ \dot{h} \end{bmatrix} = \begin{bmatrix} \frac{V_k}{(N_\mu + h)\cos\mu} \\ \frac{U_k}{M_\mu + h} \\ -\dot{W}_k \end{bmatrix} \tag{2.26}$$

where M_μ and N_μ are defined as follows [23]

$$M_\mu = N_\mu . \frac{1 - e^2}{1 - e^2 \sin^2\mu} \tag{2.27}$$

$$N_\mu = \frac{a}{\sqrt{1 - e^2 \sin^2\mu}} \tag{2.28}$$

where constant values are [23]

$$a = 6378137.0\, m \tag{2.29}$$

$$f = 0.0034\,[1] \tag{2.30}$$

$$e = 0.0818\,[1] \tag{2.31}$$

and conversion from forces in Body fixed frame to forces in Earth fixed frame is given as follows

$$\begin{bmatrix} U_k \\ V_k \\ W_k \end{bmatrix} = M_{ob} \begin{bmatrix} u \\ v \\ w \end{bmatrix} \tag{2.32}$$

where the transformation matrix M_{ob} is [5]:

$$M_{ob} = \begin{bmatrix} \cos\psi\cos\theta & \cos\psi\sin\theta\sin\phi - \sin\psi\cos\phi & \cos\psi\sin\theta\cos\phi + \sin\psi\sin\phi \\ \sin\psi\cos\theta & \sin\psi\sin\theta\sin\phi + \cos\psi\cos\phi & \cos\psi\sin\psi\sin\theta\cos\phi - \cos\psi\sin\phi \\ -\sin\phi & \cos\theta\sin\phi & \cos\theta\cos\phi \end{bmatrix} \tag{2.33}$$

2.9 Characteristics of an airplane

Table 2.1 shows mass and dimensional characteristics of the airplane which were used in the simulation:

Table 2.1: Mass and dimensional characteristics of modelled airplane [22]

Constant	Value
m	$9295.44\,kg$
I_X	$12875\,kg.m^{-2}$
I_Y	$75674\,kg.m^{-2}$
I_Z	$85552\,kg.m^{-2}$
I_{XZ}	$1331\,kg.m^{-2}$
H_e	$216.9\,kg.m^{-2}$
b	$9.45\,m$
S	$27.87\,m^2$
$\bar{c}$	$3.45\,m$
$X_{cg,ref}$	$0.35\bar{c}$
X_{cg}	$0.35\bar{c}$
δ_h limit	$\pm 25\,deg$
δ_a limit	$\pm 21.5\,deg$
δ_r limit	$\pm 30\,deg$
$\delta_l ef$ limit	$25\,deg$
$\delta_s b$ limit	$60\,deg$

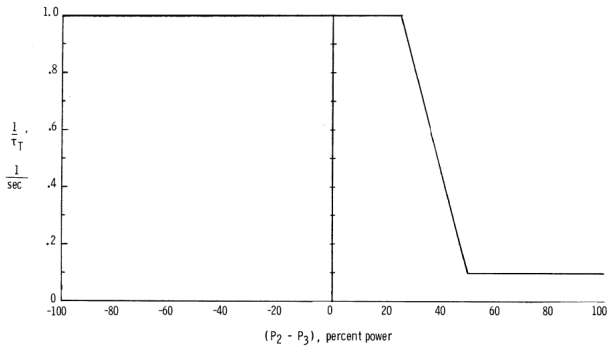

Figure 2.5: Variation of inverse thrust time constant [22]

2.10 Propulsion

A model of the propulsion unit is based on the data provided in [22]. The amount of thrust generated by the propulsion unit is calculated according to the logic diagram shown in figure A.1. The input of the diagram, P_1, is based on the position of throttle stick according to figure 2.6, function f is shown in figure 2.5 and T_{idle}, T_{mil} and T_{max} are values from table 2.2. The engine angular momentum was modelled as a constant (value can be found in 2.1 [22].

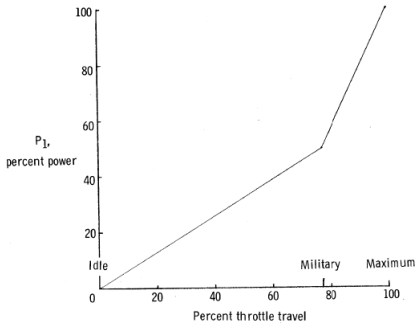

Figure 2.6: Power variation with throttle position [22]

Table 2.2: Thrust values [22]

$h\,[m]$	**0**	**3 048**	**6 096**	**9 144**	**12 192**	**15 240**
P_1	$T_{idle}\,[N]$					
0.2	2 824	1 890	3 069	4 492	5 916	7 562
0.4	267	111	1 535	3 358	5 026	6 783
0.6	-4 537	-3 158	-1 334	1 557	4 048	6 049
0.8	-12 010	-8 451	-5 782	-1 099	2 669	4 893
1.0	-16 013	-6 227	-2 647	-1 521	-890	3 114
P_1	$T_{mil}\,[N]$					
0.2	56 401	40 699	28 080	17 970	10 987	6 227
0.4	56 089	41 420	29 401	19 082	11 565	6 939
0.6	56 223	43 764	31 536	20 728	12 632	7 384
0.8	55 111	45 263	34 472	23 663	14 456	8 585
1.0	51 953	43 804	35 806	27 133	16 902	10 275
P_1	$T_{max}\,[N]$					
0.2	95 276	69 834	49 929	32 573	19 727	11 565
0.4	100 970	74 993	54 489	36 269	22 240	12 610
0.6	107 820	84 112	61 204	41 300	25 354	14 300
0.8	115 959	93 742	73 057	49 440	30 513	17 570
1.0	128 485	103 723	81 398	59 997	38 440	22 494

2.11 Actuator Model

The actuators of the control surfaces were modelled according to the data provided in [22].

The elevator actuator has been modelled as a first-order lag of $0.0495s$, with a rate limit of $60°.s^{-1}$ and a deflection limit of $25°$.

The aileron actuator has been modelled as a first-order lag of $0.0495s$, with a rate limit of $80°.s^{-1}$ and a deflection limit of $\pm 21.5°$.

The rudder actuator has been modelled as a first-order lag of $0.0495s$, with a rate limit of $120°.s^{-1}$ and a deflection limit of $\pm 30°$.

The description of the leading-edge flap actuator as well as an example of implementation of an actuator is provided in 4.4.

3. Non-linear Flight Control System Theory

In order to control system like the F-16 model described in chapter 2, two basic control strategies exist: linear or non-linear controller [28]. As the F-16 model is non-linear [29], the linear controller would have to rely on linearization of the non-linear model which would only be an approximation of the original system near the reference point. The accuracy of such approximation decreases if the condition of the system deviates from solution, thus lowering the performance of the controller [28].

Non-linear controllers, according to [28], offer several advantages:

- Improvement of the existing system
- Analysis of non-linearities
- Dealing with the model uncertanities
- Design simiplicity

3.1 Non-linear controller design methods

As there is not available a general method for designing a non-linear control system [28], a basic description of several possible approaches will be shown.

3.1.1 Gain-scheduling

The gain-scheduling is based on an idea of selecting multiple operating points, which cover the whole operating area. For each one of these points, a linear approximation of the non-linear system is made and, subsequently, a linear feedback controller for this approximation. Parameters of different controllers between operating points are interpolated. The disadvantages of this approach are the complexity in deriving formal proof of the stability of the controller, inflexible design and tedious selection of operating points and designing controllers for each of them. However, despite these disadvantages, gain-scheduling is widely used in aerospace and process control [17].

3.1.2 Nonlinear Dynamic Inversion

The non-linear dynamic inversion (NDI) approach is also related to as feedback linearization. It is based on transforming a non-linear system to an equivalent linear system through a non-linear state feedback. The output of this process is one linear system, which can be controlled by only one controller, thus no gain-scheduling is needed. The disadvantage of

the NDI lies in a fact that it relies on exact cancellation of the non-linearities in the system. The model uncertainties or changes of its parameteres may occur in complex systems (like aircraft). Because of this, an exact cancellation of non-linearities may become impossible, which affects the controller performance. However, the NDI is widely used in aerospace and is believed to eventually replace gain-scheduling as the most popular approach to non-linear control [9].

3.1.3 Backstepping

Backstepping can be applied to systems which are not feedback linearizable or can be used in order to gain more flexibility in the controller design. This method is based on a recursive method which starts with differential equations of the non-linear system and steps back towards control inputs which are separated from them by the largest number of integrators. For each recursive step a stabilizing feedback is constructed [30].

3.1.4 Robust Control

The robust control law can be used as an auxiliary linear controller of a non-linear system to assure robustness of the controller in case some disturbances (measurement noise, unmodelled dynamics) occur. However, if the uncertainties become larger or are unknown, it may result in an overly conservative approach or a fail to provide adequate response of the system [28].

3.1.5 Adaptive Control

Then adaptive control has been developed as an alternative approach to deal with uncertain or time-varying systems. The adaptive control can, as the name suggests, adapt to changes in the controlled system. To achieve this, it increases the order of the controller. A standard way to implement adaptive control is to use artificial neural networks, although they make the process of the certification of such control system difficult as it is non-trivial to prove that the adaptive control will not learn incorrectly or that it would assure stability of the system in case of a failure in the adaptation to an extreme level [28].

3.1.6 Incremental Control

The incremental control is a modification which can be applied to both backstepping and non-linear dynamic inversion. In this modification, an acceleration feedback is used to extract the information relative to any aerodynamic change of the aircraft. Moreover, to achieve the desired result the controller only computes the incremental changes with respect to the previous changes rather than computing total control inputs. In case of modifying the NDI controller, the main advantage is that because of its incremental derivation, the controller does not need data that depend exclusively on the states of the system, which enhances robustness of the control law [3].

3.2 Non-linear Dynamic Inversion

As the created flight control system (chapter 4) uses the Non-linear Dynamic Inversion, further description will focus in detail on this approach The following section is based on [26].

3.2.1 Theoretical background

The Non-linear Dynamic Inversion allows to generate a control input using the non-linear feedback control and state transformation, which, when applied, the relation between virtual control input $\dot{\gamma}$ and the output of the system becomes linear. After that, a linear control law for $\dot{\gamma}$ can be designed.

Please note that while it is common to use symbol $\dot{\mu}$ for the virtual control input, $\dot{\mu}$ is used as a symbol for latitude in this thesis, and therefore symbol $\dot{\gamma}$ is used for the virtual control input instead.

To show it mathematically, consider this n-order non-linear SISO (Single input single output) system:

$$\frac{\partial^n x_1}{\partial^n t^n} = b(x) + A(x)u \tag{3.1}$$

$$y = h(x) = x_1 \tag{3.2}$$

where x is state vector in R^n, u is a scalar input and A and b are scalar functions from R^n to R.

This system can be recast to a companion matrix form:

$$\frac{\partial}{\partial t} = \begin{bmatrix} x_1 \\ \vdots \\ x_{n-1} \\ x_n \end{bmatrix} = \begin{bmatrix} x_2 \\ \vdots \\ x_n \\ b(x) + A(x)u \end{bmatrix} \tag{3.3}$$

We can also see explicit dependency on the control input, so if the virtual control input is defined as:

$$\dot{\gamma} = \frac{\partial x_n}{\partial t} = \frac{\partial^n y}{\partial t^n} = b(x) + A(x)u \tag{3.4}$$

when $A(x) \neq 0$ it is possible to solve for control input:

$$u = A(x)^{-1}(\dot{\gamma} - b(x)) \tag{3.5}$$

and if we introduce this expression to the companion matrix form, we get:

$$\frac{\partial}{\partial t} = \begin{bmatrix} x_1 \\ \vdots \\ x_{n-1} \\ x_n \end{bmatrix} = \begin{bmatrix} x_2 \\ \vdots \\ x_n \\ \dot{\gamma} \end{bmatrix} \tag{3.6}$$

where all non-linearities are cancelled and system can be represented by a sequence of integrators.

4. Implemented Flight Control System

The flight control system implemented for the modelled airplane consists of four parts: pitch control system, roll control system, yaw control system and leading-edge flap control system. While the latter three were implemented according to their description and diagrams provided in [22], a new flight control system based on Non-linear Dynamic Inversion has been developed for the pitch control, capable of reaching and maintaining the desired angle of attack with manually operated or fixed throttle stick position.

4.1 Deriving equations for the pitch control system

Firstly, as the implemented flight control system controls only part of the whole system (in our case it is the pitch motion), it is necessary to define which equations of the model are related to the pitch motion and thus need to be „controlled“ using the Non-linear Dynamic Inversion (which was described theoretically in chapter 3). After that, these equations must be transformed to the following form:

$$\dot{\gamma} = A(x)u + b(x) \tag{4.1}$$

where $\dot{\gamma}$ is the virtual control input, u is the controlled output, A and b are scalar functions from R^n to R and x is state vector in R^n. Transforming this form, equation of the output is:

$$u = A(x)^{-1}(\dot{\gamma} - b(x)) \tag{4.2}$$

4.1.1 Angle of Attack

As the pitch movement is basically done by changing the Angle of Attack of an airplane, the first equation will be the equation of Angle of Attack. This equation will be the outer loop of the entire NDI controller (see figure 4.2). An equation used in the simulation was presented in section 2.8.1, however, for the purposes of the inversion, following equation has been used, which can be derived from the original one (2.13) [8]:

$$\dot{\alpha} = \frac{Z_T}{mV\cos\beta} - (p\cos\alpha + r\sin\alpha)\tan\beta + q \tag{4.3}$$

where

$$Z_T = \frac{\overline{q}S}{m}C_{Z,t}$$

which is a term of the equation of airplane acceleration along Z body axis (2.3), where $C_{Z,t}$ is the aerodynamic coefficient defined in the section 2.7 (equation 2.8). It is now necessary to transform the equation 4.3 to the equation 4.2, where u will be q, $\dot{\gamma}$ will be $\dot{\alpha}$ and $A(x)$ and $b(x)$ will be as described in section 4.1. To achieve that, we need to isolate q in the equation

and define $A_o(x)$ and $b_o(x)$ (where subscript $_o$ stands for outer). As the equation including $C_{Z,t}$ is rather long and complicated, a solution will be provided in partial description+.

Isolating q and defining $A_o(x)$ and $b_o(x)$

There are two occurrences of q in the whole equation. Further occurrences of the symbol q will be referred to as q_c ($_c$ stands for command), because in this section we use the pitching moment as a value commanded by the control system and not the value computed by the aircraft dynamic model. It is present as an independent term in equation 4.3 and also as a part of the last term in the $C_{Z,t}$ equation:

$$C_{ZQ} = \frac{\bar{c}q}{2V}\left[C_{Z_q}(\alpha) + \Delta C_{Z_{q,lef}}(\alpha)\left(1 - \frac{\delta_{lef}}{25}\right)\right] \tag{4.4}$$

Let the 4.4 be C_{ZQ} and let the rest of the $C_{Z,t}$ equation be $C_{Z,rest}$. Then the whole equation would be:

$$\dot{\alpha} = \frac{\frac{\bar{q}S}{m}C_{ZQ} + \frac{\bar{q}S}{m}C_{Z,rest}}{mV\cos\beta} - (p\cos\alpha + r\sin\alpha)\tan\beta + q_c \tag{4.5}$$

which can be transformed into:

$$\dot{\alpha} = \frac{\bar{q}SC_{ZQ}}{m^2V\cos\beta} + \frac{\bar{q}SC_{Z,rest}}{m^2V\cos\beta} - (p\cos\alpha + r\sin\alpha)\tan\beta + q_c \tag{4.6}$$

and to make $b_o(x)$ clear:

$$\dot{\alpha} = \frac{\bar{q}SC_{ZQ}}{m^2V\cos\beta} + q_c + \frac{\bar{q}SC_{Z,r}}{m^2V\cos\beta} - (p\cos\alpha + r\sin\alpha)\tan\beta \tag{4.7}$$

As the q_c only occurs in first two terms, we can conclude, that the rest of the equation will be $b_o(x)$:

$$b_o(x) = \frac{\bar{q}SC_{Z,r}}{m^2V\cos\beta} - (p\cos\alpha + r\sin\alpha)\tan\beta \tag{4.8}$$

It is now necessary to isolate q_c from the first two terms. Firstly, let's substitute C_{ZQ} for the term it represents:

$$\dot{\alpha} = \frac{\bar{q}S\frac{\bar{c}q_c}{2V}\left[C_{Z_q}(\alpha) + \Delta C_{Z_{q,lef}}(\alpha)\left(1 - \frac{\delta_{lef}}{25}\right)\right]}{m^2V\cos\beta} + q_c + b_o(x) \tag{4.9}$$

We can now isolate q_c:

$$\dot{\alpha} = q_cA_o(x) + b_o(x) \tag{4.10}$$

where $A_o(x)$ is:

$$A_o(x) = \frac{\bar{q}S\bar{c}\left[C_{Z_q}(\alpha) + \Delta C_{Z_{q,lef}}(\alpha)\left(1 - \frac{\delta_{lef}}{25}\right)\right]}{2m^2V^2\cos\beta} + 1 \tag{4.11}$$

And if we isolate q_c in equation 4.10, we reach the desired form, where q_c stands for u and $\dot{\alpha}$ stands for $\dot{\gamma}$:

$$q_c = A_o(x)^{-1}(\dot{\alpha} - b_o(x)) \tag{4.12}$$

4.1.2 Pitching moment

While the angle of attack defines the airplane's position relative to the oncoming air, it is the pitching moment, which defines airplane's motion along its pitch axis. The pitching moment equation was presented in section 2.6.2 (equation 2.5), with $C_{m,t}$ defined in equation 2.9. This equation will be the inner loop of the NDI controller (see figure 4.2) and needs to be transformed the same way as the Angle of Attack equation. The input, $\dot{\gamma}$ will be $\dot{q}$ and the output will be δ_h as the deflection of the elevator controls the airplane's motion along the pitch axis. As in the previous case, we need to define $A_i(x)$ and $b_i(x)$, where subscript $_i$ stands for inner.

Isolating δ_h and defining $A_i(x)$ and $b_i(x)$

Concerning the equations of $\dot{q}$ (2.5) and $C_{m,t}$ (2.9), we can see, that δ_h is only present in the latter one in the first and last term. As the last term contains aerodynamic data for deep stall, which is rather non-standard flight regime and is not the goal of this thesis to create flight controller for deep stall conditions, this could be neglected and only first term is taken into consideration for isolating δ_h, which looks as follows:

$$C_m(\alpha, \beta, \delta_h)\eta_{\delta_h}(\delta_h) \tag{4.13}$$

Apart from the Angle of Attack, where q was directly in the equation, in this case δ_h does not stand alone and is only used as a parameter. The first factor of this product is three-dimensional table, which is made from five two dimensional tables (in other words, five two dimensional layers). The two dimensions in each table are α and β and each of these tables is valid for a different value of δ_h. Values between the tabulated values are interpolated. The second factor is an effectiveness coefficient, described by one-dimensional table with almost all values equal to 1. As we need to isolate δ_h, it is necessary to substitute this product for another expression, where δ_h would be present directly. After analyzing the

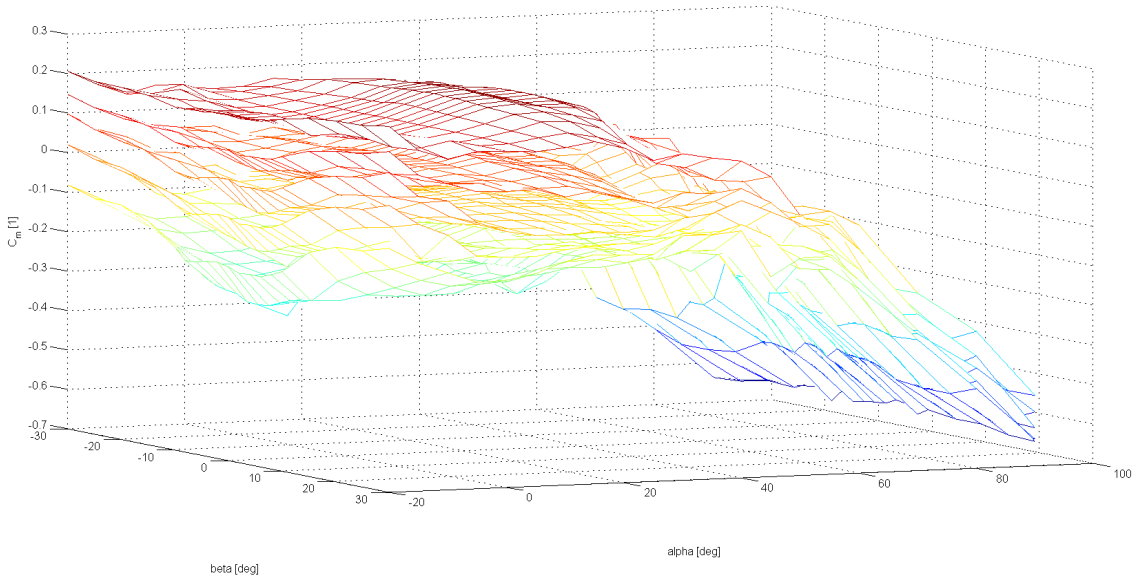

Figure 4.1: $C_m(\alpha, \beta, \delta_h)$ table

three dimensional table and its data (figure 4.1), following substitution has been created:

$$C_m(\alpha, \beta) + \delta_h C_{m_{\delta_h}} \tag{4.14}$$

where $C_m(\alpha, \beta)$ represents data valid for $\delta_h = 0°$, which serve as a base value and $C_{m_{\delta_h}}$ is a coefficient used to compute table values for specific values of δ_h. This substitution is based on the observation, that the five layers of the table are approximately evenly distant from each other, and therefore, if a value is known for certain α, β and δ_h, value for the same α and β, but different δ_h can be computed from this value using substitution 4.14, if a proper coefficient is found.

The actual computation of the $C_{m_{\delta_h}}$ coefficient is rather straightforward. It has been done by finding values for the same α and β in different δ_h layers, computing the difference between the values and then computing the assumed difference for $\Delta\delta_h = 1°$, which is done by a simple division. This has been repeated for several pairs of values to compute the average value of the coefficient and to reduce the possible error. The obtained value of $C_{m_{\delta_h}}$ is -0.010235 [1].

Please note, that in the following equations δ_h symbol will be substituted for $\delta_{h,c}$ as it is the value commanded by the controller and not the deflection of the elevator itself.

If we mark the rest of the $C_{m,t}$ equation as $C_{m,rest}$ (the equation without the first term) the whole equation would be:

$$\dot{q} = \frac{I_Z - I_X}{I_Y} pr + \frac{I_{XZ}}{I_Y}(r^2 - p^2) + \frac{\bar{\mathrm{q}} S \bar{\mathrm{c}}}{I_Y}\left(C_m(\alpha, \beta) + \delta_{h,c} C_{m_{\delta_h}}\right) + \frac{\bar{\mathrm{q}} S \bar{\mathrm{c}}}{I_Y} C_{m,rest} - \frac{H_e r}{I_Y} \tag{4.15}$$

Next, since $\delta_{h,c}$ is present only in one term, we can easily indentify remaining terms which belong to $b_i(x)$:

$$b(x) = \frac{\bar{\mathrm{q}} S \bar{\mathrm{c}}}{I_Y} C_m(\alpha, \beta) + \frac{\bar{\mathrm{q}} S \bar{\mathrm{c}}}{I_Y} C_{m,r} + \frac{I_Z - I_X}{I_Y} pr + \frac{I_{XZ}}{I_Y}(r^2 - p^2) - \frac{H_e r}{I_Y} \tag{4.16}$$

so the equation with $b_i(x)$ would be:

$$\dot{q} = \frac{\bar{\mathrm{q}} S \bar{\mathrm{c}}}{I_Y} \delta_{h,c} C_{m_{\delta_h}} + b_i(x) \tag{4.17}$$

now if we change the order of multiplicands in the first term, we can define $A_i(x)$:

$$\dot{q} = A_i(x)\delta_{h,c} + b_i(x) \tag{4.18}$$

where $A_i(x)$ is:

$$A_i(x) = \frac{\bar{\mathrm{q}} S \bar{\mathrm{c}}}{I_Y} C_{m_{\delta_h}}$$

And if we isolate $\delta_{h,c}$ in equation 4.18 we reach the desired form, where $\delta_{h,c}$ stands for u and $\dot{q}$ stands for $\dot{\gamma}$:

$$\delta_{h,c} = A_i(x)^{-1}(\dot{q} - b_i(x)) \tag{4.19}$$

4.2 NDI Implementation

Having the equations derived, the next step is to implement them to control the created aerodynamic model. A method called cascaded non-linear dynamic inversion (also known as non-linear dynamic inversion using time scale separation) has been chosen for implementation. In this method, the system is divided into two loops: inner and outer, where the dynamics of the inner loop has to be faster than the dynamics of the outer loop [14]. The scheme of the inner and the outer loop of a cascaded non-linear dynamic inversion used

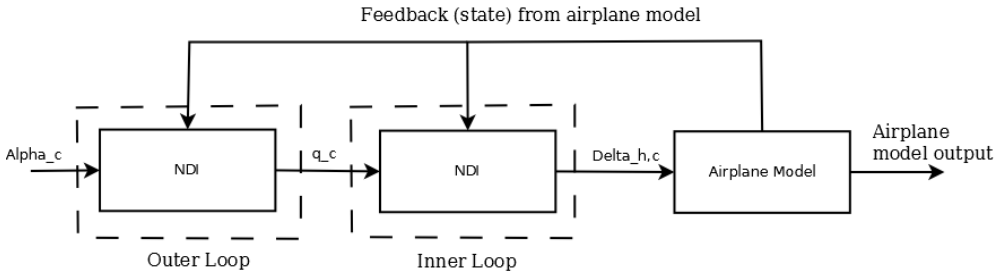

Figure 4.2: The scheme of cascaded NDI used in simulation

in simulation is shown in figure 4.2. The NDI blocks consists of three parts: the reference model, the PI controller and the computation of the output. The scheme of the NDI block is provided in figure 4.3. Measured input is of course not measured but computed in the model, but the name „measured“ was used in order to comply with the standard marking.

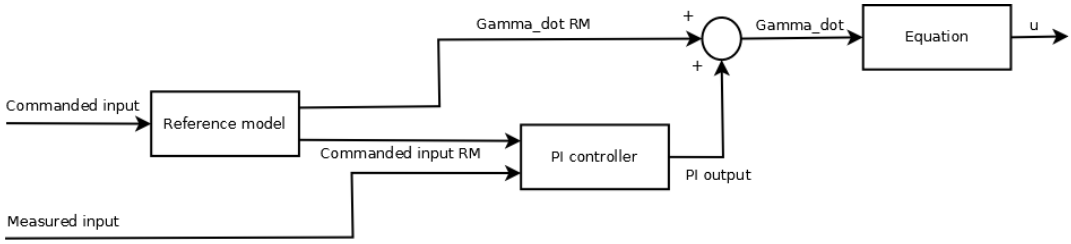

Figure 4.3: Scheme of the NDI block

4.2.1 Reference Model

The reference model is used to transform the input (in other words, desired output of the airplane model) into commanded variable called virtual control input handed into the rest of the sytem [19] and it also provide a reference value for a PI controller. The reference model determines „how fast“ the controller reacts to a change of the value of the virtual control input. This behaviour is controlled by a value of T_s constant. The scheme of implemented reference model is shown in figure 4.4.

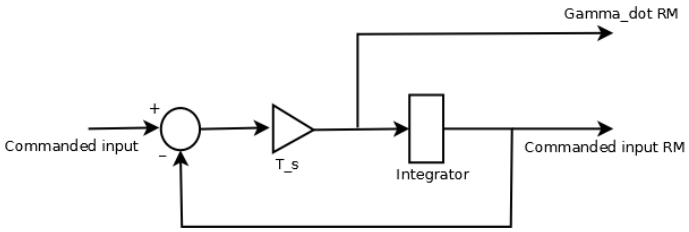

Figure 4.4: Scheme of the reference model

4.2.2 PI controller

The PI (proportional-integral) controller is used to compute the difference between the desired value of the output of the airplane model and the actual value measured (but in

this case, of course, computed in the model). After that, the PI controller tries to minimize the difference using manipulated variable, which consists of proportional and integral term. These terms can be controlled through tuning proportional (K_p) and integral gain (K_i) [24]. The scheme of the PI controller is shown in figure 4.5.

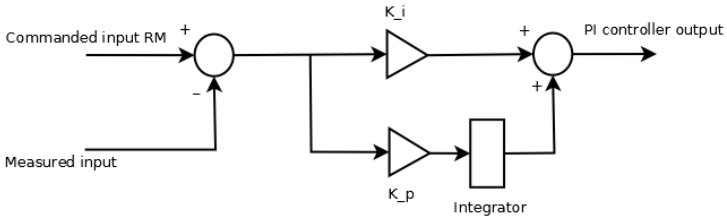

Figure 4.5: Scheme of the PI controller

4.2.3 Tuning the coefficients

The performance of both reference model and PI controller depends significantly on the values of their coefficients. Unfortunately, even though some rules for tuning the coefficients exists, the majority of the work is still done by trial and error method [24]. Nonetheless, after testing multiple values and combinations, coefficients, which provide satisfactory results were found and can be found in table 4.1.

Table 4.1: Reference model and PI controller coefficients

Gain	**Value**	
	Outer loop	Inner loop
T_s	1	6
K_p	7	0.05
K_i	4	0.03

4.2.4 Actuator Model

As the control system operates the elevator (in other words, it computes the needed deflection) it is also necessary to model the actuator, which physically operates the elevator in real airplane. The actuator was modelled using values from [22]: first-order lag of 0.0495s, rate limit of $25°.s^{-1}$ and maximum deflection of 25°. The implementation of the actuator is show in figure 4.6

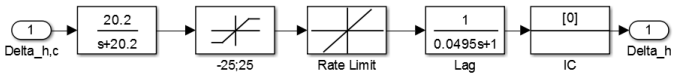

Figure 4.6: Actuator model

4.3 Roll and yaw control system

Flight control systems for roll and yaw axis were implemented according to the description provided in [22]. The implementation also incorporates changes to the basic flight control

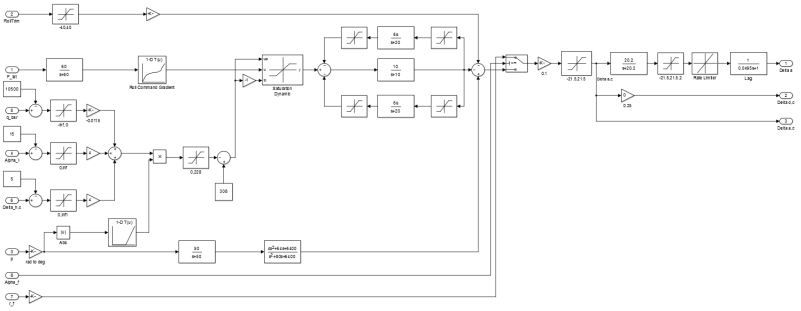

Figure 4.7: An overall scheme of the roll control system as implemented in Simulink

systems and also contain actuator models as described in [22]. The overall scheme of the roll figure control system is shown in figure 4.7 and the overall scheme of the yaw figure control system is shown in figure 4.8.

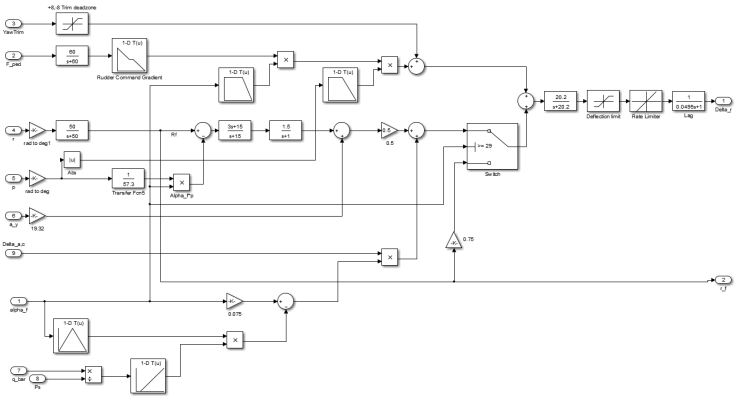

Figure 4.8: An overall scheme of the yaw control system as implemented in Simulink

4.4 Leading-edge flap control system

Leading-edge flap deflection is computed using equation 4.20 and actuator was modelled as first-order lag of 0.136s with rate limit of $25°.s^{-1}$ and a maximum deflection 25° [22]:

$$\delta_{lef} = 1.38\frac{2S + 7.25}{S + 7.25}\alpha - 9.05\frac{\bar{q}}{P_s} + 1.45 \tag{4.20}$$

5. Results

This chapter provides the results of the simulation of the pitch control system response (see chapter 4 for detailed description of the system). The pitch control system is capable of reaching and maintaing commanded angle of attack (α) by deflecting the elevator, if the flight parameteres allow so, as this system controls only the motion about one axis of the airplane and also does not control thrust of the engine. Therefore, fixed position of throttle stick or a manual control of the throttle stick is assumed.

As the amount of the test cases is potentially infinite, an example of the work of the pitch control system will be presented.

5.1 Initial conditions

Table 5.1 summarizes the initial conditions of the simulation, which were set to a steady level flight at altitude $5000\,m$ with the initial speed $150\,m.s^{-1}$. All other state variables are zero. The time of the simulation is set to thirty seconds.

Table 5.1: Initial conditions of the simulation

Variable	**Value**
u	$150\,m.s^{-1}$
v	$0\,m.s^{-1}$
w	$0\,m.s^{-1}$
p	$0\,rad.s^{-1}$
q	$0\,rad.s^{-1}$
r	$0\,rad.s^{-1}$
θ	$0\,deg$
ϕ	$0\,deg$
ψ	$0\,deg$
α	$0\,deg$
β	$0\,deg$
h	$5000\,m$

5.2 Outer loop

The control system is set to maintain the Angle of Attack at zero. After the initial five seconds of the simulation, the system is commanded to reach and maintain an Angle of Attack of $5°$ ($\alpha_c = 5°$). Following figures demonstrate the result. Figure 5.1 shows graph of

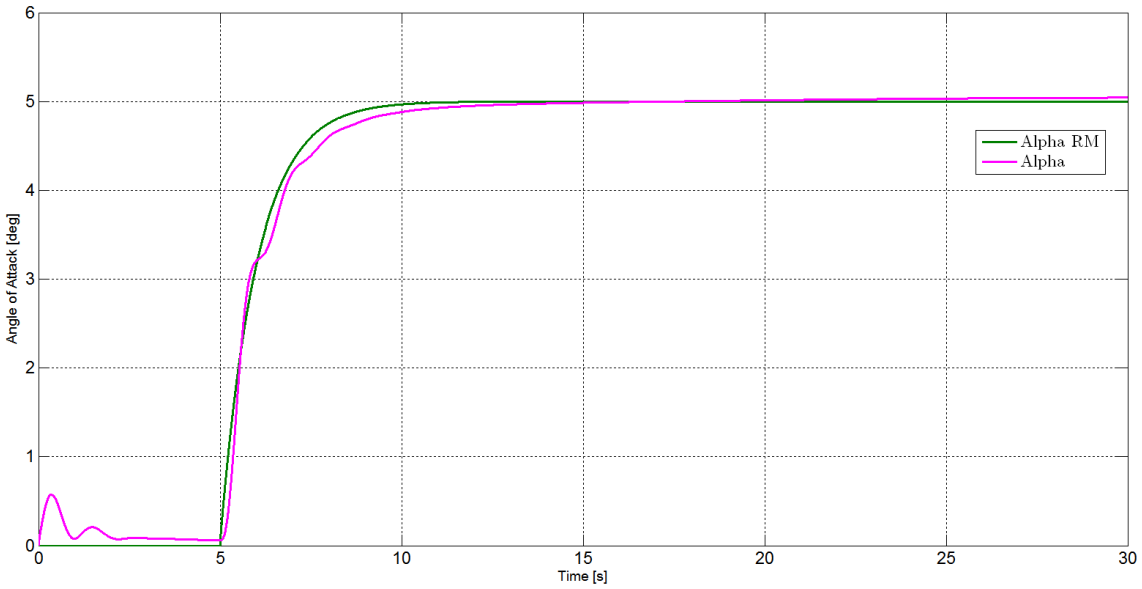

Figure 5.1: α_{RM} and α graph ($\alpha_c = 5°$

α_{RM} (yellow, output of reference model) and α (purple, computed in this case, measured in real system).

The rise of α in the beginning is caused by the initial conditions, where the aircraft has zero pitch angle and starts descending because of a low angle of attack and speed. As the pitch angle is still close to zero, this causes the value of Angle of Attack to rise. However, the pitch control system manages to lower the angle of attack almost to zero within the first five seconds. At the five second mark, it is commanded to increase the Angle of Attack to five degrees and mantain it. The graph shows that the real angle of attack which is controlled by control system closely follows the desired values with minimal errors. The biggest difference between the two is between the 5^{th} and 10^{th} second, which is a standard behaviour of PI controllers. Although it is possible to reach desired value faster, it is for the price of bigger overshoot and oscillations.

5.2.1 Example of using different coefficients

During the development, a behaviour with different coefficients has been also investigated. Figure 5.3 shows an example of the result with one considered combination. Values of coefficients can be found in table 5.2. Bigger overshoot and oscilations of α can be seen as mentioned in previous paragraph. It also took longer to reach the desired value.

Table 5.2: Values of coefficients used during the development of the control system

Gain	**Value**	
	Outer loop	Inner loop
T_s	1	1
K_p	5	0.05
K_i	2	0.03

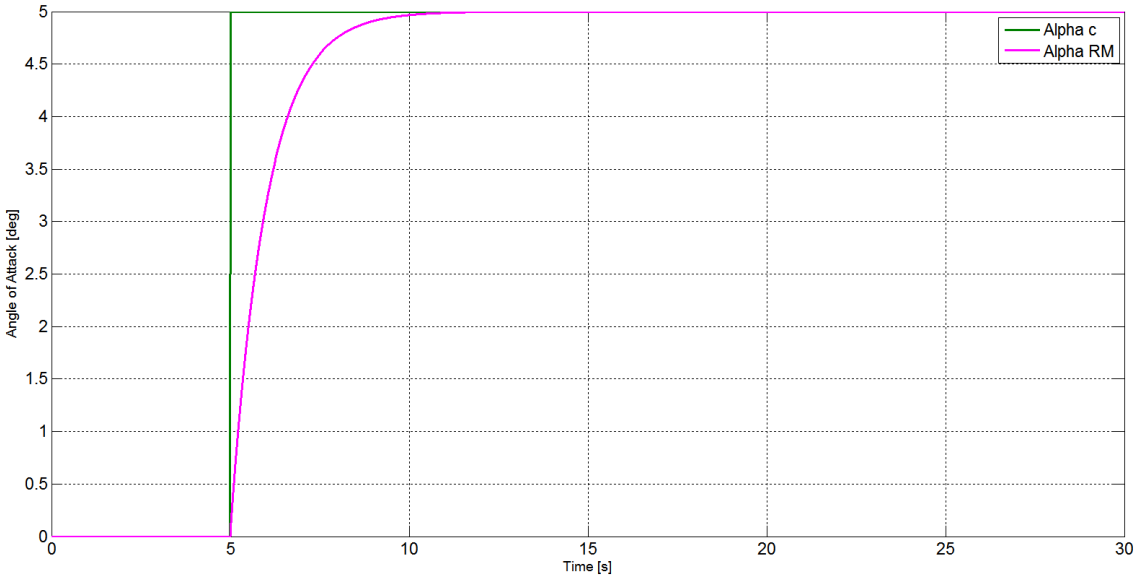

Figure 5.2: Reference model response to the change of α_c

5.2.2 Changing value of α_c during simulation

To prove the controller has the ability to decrease the Angle of Attack a test of such command has been conducted. The figure 5.4 shows a behaviour of the system, which received two commands: reach and maintain angle of attack at 5° ($\alpha_c = 5°$) from the 5^{th} second onwards and reach and maintain angle of attack at 3° ($\alpha_c = 3°$) from the 15^{th} second onwards.

5.3 Inner loop

The inner loop of the system deals with pitching moment (q). The desired behaviour in this case is pitching moment commanded by the outer loop (q_c), where it is computed in equation block (see figure 4.3) according to commanded angle of attack.

The figure 5.5 shows input (q_c) and output (q_{RM}) of the reference model of the inner loop (T_s constant is 6). As we can see, the reference model is not able to reach „extreme, but short“ changes of value, as the value drops before it is able to do so, however, this behaviour is understandable as the non-zero reaction time will always cause such behaviour (at least to some extent).

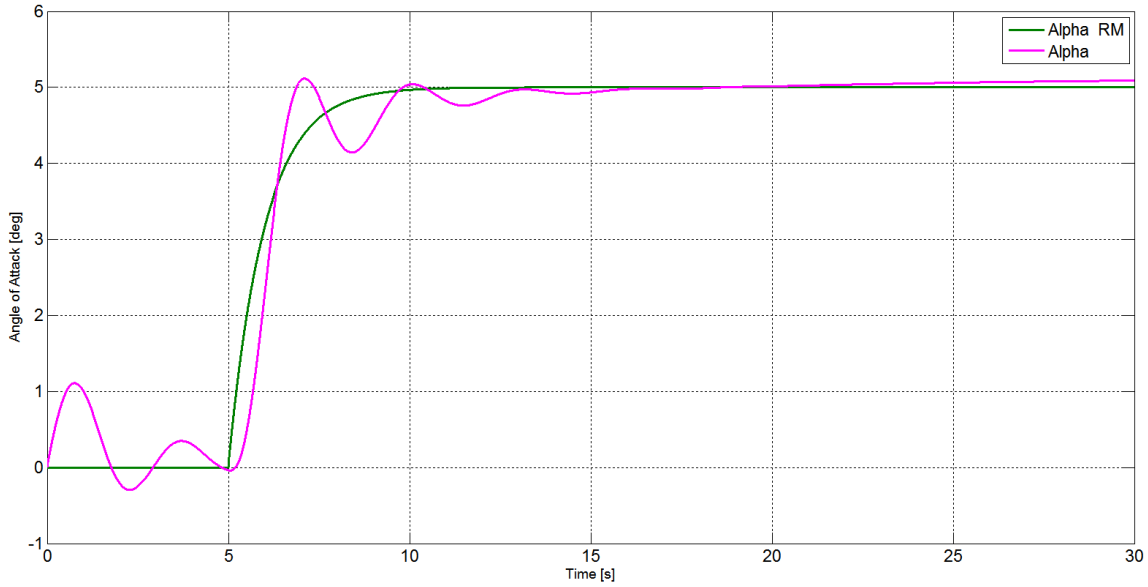

Figure 5.3: α_{RM} and α graph ($\alpha_c = 5°$, second test case)

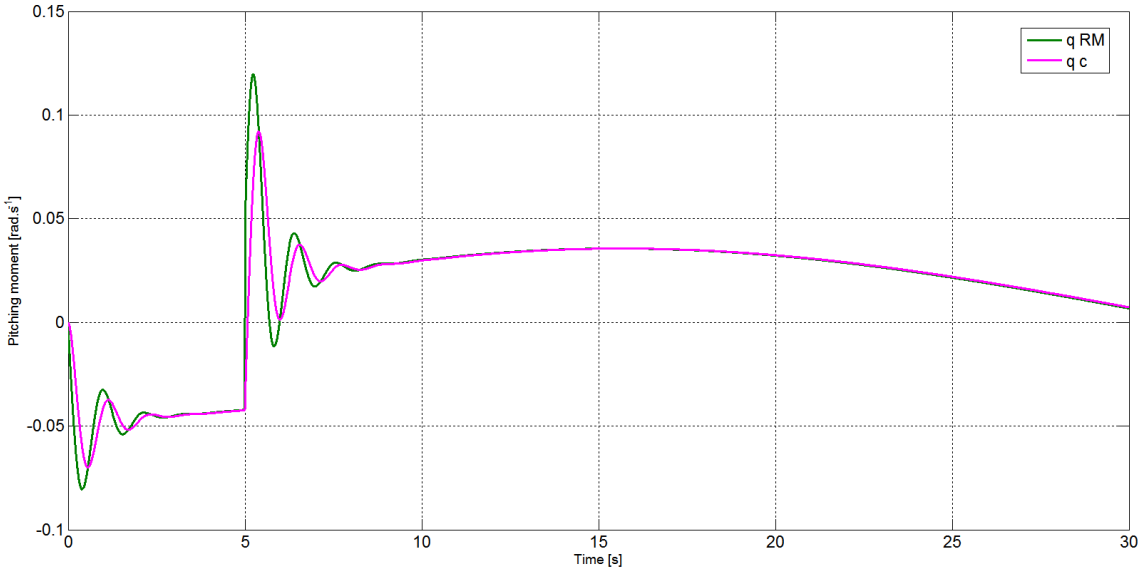

Figure 5.5: q_{RM} and q_c graph

The figure 5.6 shows relationship between q_{RM} and q (two inputs of the PI controller in the inner loop). As we can see, the error is between the reference model value and „real“ value of the system is less than $0.01\,rad/s$

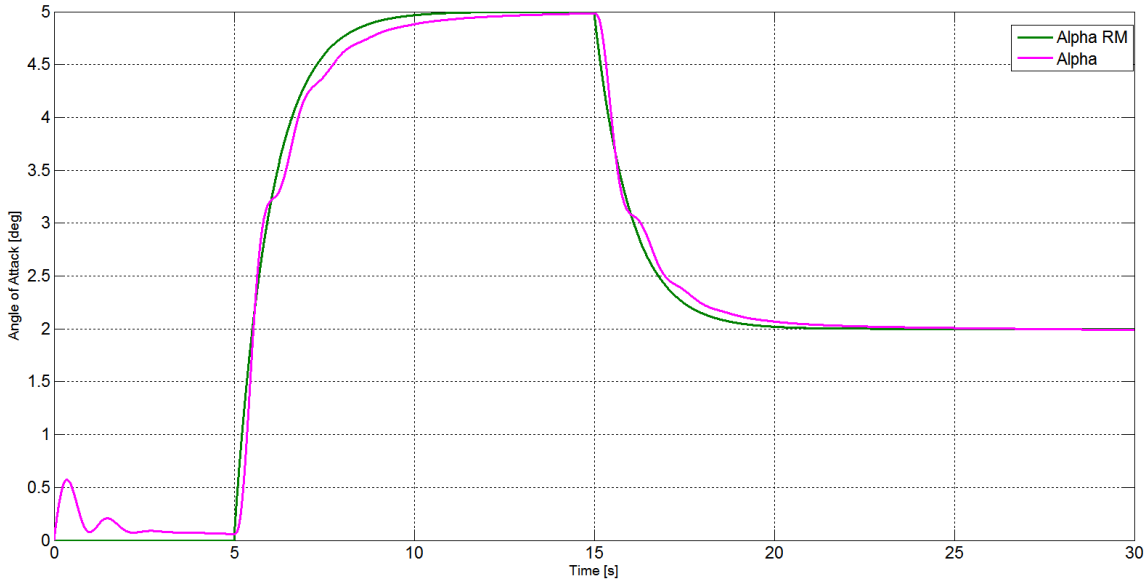

Figure 5.4: α_{RM} and α graph, changing value of α_c

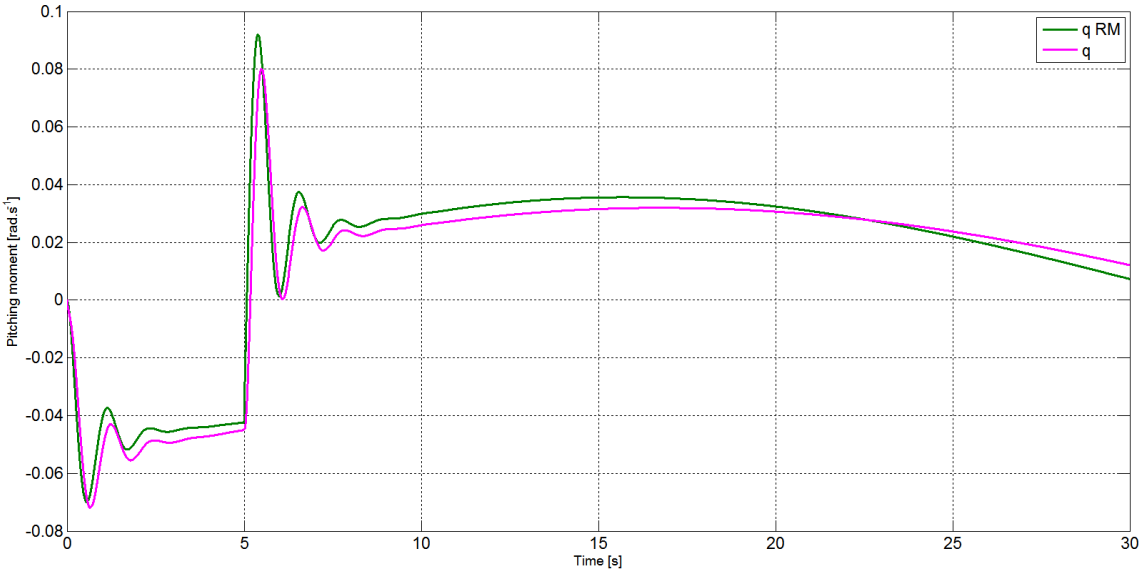

Figure 5.6: q_{RM} and q graph

5.4 Deflection of the elevator

The output of the controller is the deflection of the elevator ($\delta_{h,c}$) and is then used as an input of the actuator model (4.2.4), which transform it into the deflection of the elevator shown in figure 5.7. This figure corresponds to the first test case ($\alpha_c = 5^{th}$ second onwards).

The controller commanded positive deflection of the elevator (the deflection is positive for airplane nose-down control) in the 1^{st} second to decrease the Angle of Attack (as the desired Angle of Attack is 0 at the start of the simulation). At the 5^{th} second mark, the controller comanded negative deflection of the elevator to increase the Angle of Attack to 5°. The subsequent oscillation is caused by the controller trying to stabilize the Angle of

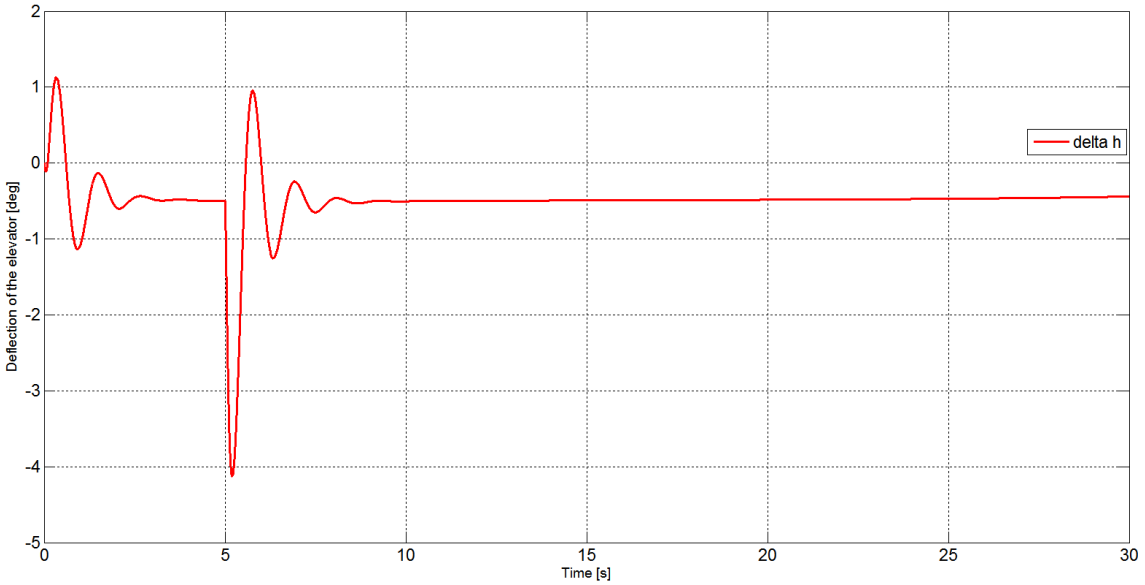

Figure 5.7: δ_h deflection

Attack and from the 8^{th} second onwards, the deflection of the elevator is stable in order to maintain the commanded Angle of Attack.

6. Potential Future Improvements

While the achvieved results are satisfactory, there is still a room for improvements. Some of them are:

- As the current NDI control system controls only the pitch pitch motion, the next step would be creating and implementing an NDI flight control system for all axes including thrust. The control system for the thrust would require creating equations for this system, which is currently represented by a logic diagram (in other words, this diagram and its implementation would have to be converted to equations), or it would require replacing the current thrust system by an equivalent system, from which equations for an NDI controller could be derived directly. The creation of the control system for thrust system would significantly enhance the performance of the created NDI controller, as the Angle of Attack is closely related to the speed.
- Implementing a mapping function for the position of the stick and a desired angle of attack. Currently, the desired angle of attack has to be put into the control system as a constant, but in case of finding proper mapping function, a joystick could be used, which would be more convenient.
- Enhancing the created model to cover more flight characteristics (higher speed, usage of all control surfaces) of the modelled airplane. This would require gaining additional aerodynamic data, or additional model based on blade element theory.

7. Conclusion

This bachelor's thesis deals with the modelling of a jet airplane and creating an automatic flight control system for it. It contains detailed description of equations used for the creation of the model as well as deriving the equations for the controller.

An F-16 data were used for an aerodynamic model, as the aerodynamic data for this airplane are publicly available, even though they do not cover the whole flight envelope. The F-16 is also an interesting airplane to model, as it has relaxed longitudinal stability. Even with the data and equations available, the creation of such complex model proved to be demanding and non-trivial, however, the model was succesfully implemented.

The next part of the thesis is an automatic flight control system. The flight control system for roll and yaw axis as well as control system of leading-edge flaps has been implemented according to the available description in a way, that it filters input from the pilot to ensure stability of an airplane and to ensure, that the airplane's limits like maximum angle of attack or maximum g load is not exceeded. For the pitch axis, a completely new flight control system has been created using Non-linear Dynamic Inversion and which enables fully automatic control of the Angle of Attack. Conducted tests have proved its capability of reaching and maintaining desired angle of attack, if it is physically possible.

Bibliography

[1] BIPM. *The International System of Units (SI).* Paris: Stedi Media, 8th edition, 2006. ISBN 92-822-2213-6.

[2] Guowei Cai, Ben M. Chen, and Tong Heng Lee. *Unmanned Rotorcraft Systems.* London: Springer-Verlag, Ltd., 2011. ISBN 978-0-85729-634-4.

[3] Hui B. Chen and Shuguang G. Zhang. Robust dynamic inversion flight control law design. In *Systems and Control in Aerospace and Astronautics, 2008. ISSCAA 2008. 2nd International Symposium*, 2008.

[4] The Boeing Company. What is angle of attack? *Aero*, (12), October 2000.

[5] John J. Craig. *Introduction to Robotics: Mechanics and Control.* Upper Saddle River: Pearson Education, Inc., third edition, 2005. ISBN 0-13-123629-6.

[6] Kev Darling. *Bojové legendy F-16 Fighting Falcon.* Praha: Jan Vašut, s.r.o, 2005. ISBN 80-7236-335-2.

[7] Lou Drendel. *F-16 Fighting Falcon in Action.* Carrollton: Squadron/Signal Publications, Inc., 1982. ISBN 0-89747-133-4.

[8] Eugene L. Duke, Robert F. Antoniewicz, and Keith D. Kramber. Derivation and definition of a linear aicraft model. Reference publication 1207, National Aeronautics and Space Administration Ames Research Center, 1988.

[9] Lars Sonneveldt et al. Nonlinear adaptive flight control law design and handling qualities evaluation. In *Joint 48th IEEE Conference on Decision and Control and 28th Chinese Control Conference*, 2009.

[10] Bill Guston. *The Osprey Encyclopedia of Russian Aircraft 1875-1995.* Oxford: Osprey Publishing, 2nd edition, 1995. ISBN 978-1855324053.

[11] Richard P. Hallion. *NASA's Contributions to Aeronautics*, volume 1. National Aeronautics and Space Administration, 2010. ISBN 978-0-16-084635-9.

[12] E.L. Houghton and P.W. Carpenter. *Aerodynamics for Engineering Students.* Oxford: Butterworth-Heinemann, 5th edition, 2003. ISBN 0-7506-5111-3.

[13] ISO. Standard atmosphere. ISO 2533-1975, International Organization for Standardization, Geneva, Switzerland, 1975.

[14] Mia Karlsson. Control of umnanned aerial vehicles using non-linear dynamic inversion. Master's thesis, Division of Automatic Control Department of Electrical Engineering Linköping University, December 2002. LiTH-ISY-EX-3284-2002.

[15] Wolfgang Langewiesche. *O umění létat.* Praha: Baronet a.s, 2010. ISBN 978-80-7384-307-6 [original title Stick and Rudder].

[16] T.W. Lee. *Military Technologies of the World.* Praeger Security International. ABC-CLIO, 2008. ISBN 02-7599-536-4.

[17] D.J. Leith and We. Leithead. Survey of gain-scheduling analysis design. *International Journal of Control*, 73:1001–1025, 1999.

[18] Vladimír Mertl. *Konstrukce a projektování letadel.* Number 2641. Vysoké učení technické v Brně, Fakulta strojního inženýrství, 1st edition, 2000.

[19] Christopher J. Miller. Nonlinear dynamic inversion baseline control law: Architecture and performance predictions. In *AIAA Guidance, Navigation, and Control Conference*, 2011.

[20] NASA. NASA Dryden technology facts - digital fly by wire. `https://www.nasa.gov/centers/dryden/about/Organizations/Technology/Facts/TF-2001-02-DFRC.html`, 2013-07-13 [cit. 2015-04-13].

[21] I. Newton, A. Motte, and J. Machin. *The Mathematical Principles of Natural Philosophy.* Number v. 1 in The Mathematical Principles of Natural Philosophy. B. Motte, 1729.

[22] Luat T. Nguyen et al. Simulator study of stall/post-stall characteristics of a figher airplane with relaxed longitudal stability. Technical Paper 1538, National Aeronautics and Space Administration, 1979.

[23] NIMA. Department of defense World Geodetic System 1984. Its Definition and Relationships with Local Geodetic Systems. Technical Report 8350.2, National Imagery and Mapping Agency, 2000. Third edition.

[24] Aidan O'Dwyer. *Handbook of PI and PID controller Tuning Rules.* London: Imperial College Press, 2nd edition, 2006. ISBN 1-86094-622-4.

[25] Josef Pávek and Zdeněk Kopřiva. *Konstrukce a projektování letadel I.* Ediční středisko ČVUT, 1982.

[26] S. Sieberling, Q.P. Chu, and J.A. Mulder. Robust flight control using incremental nonlinear dynamic inversion and angular acceleration prediction. *Journal of guidance, control, and dynamics*, 33(6), November-December 2010.

[27] Pedro Valério Menino Simplício. Helicopter nonlinear flight control using incremental nonlinear dynamic inversion. Master's thesis, Instituto Superior Técnico Universidade Técnica de Lisboa, October 2011.

[28] Jean-Jacques E. Slotine and Weiping Li. *Applied Nonlinear Control.* Englewood Cliffs: Prentice Hall, Inc., 1991. ISBN 0-13-040890-5.

[29] Brian L. Stevens and Frank L. Lewis. *Aircraft Control and Simulation.* Hoboken: John Wiley & Sons, Inc., 2003. ISBN 0-471-37145-9.

[30] Eduard Richard van Oort. *Adaptive Backstepping Control and Safety Analysis for Modern Fighter Aircraft.* PhD thesis, Delft University of Technology, 2011.

[31] Michael Wilson. RAE Electric Hunter. *Flight International*, 103(3355), 28 June 1973.

A. Logic diagram of the thrust system

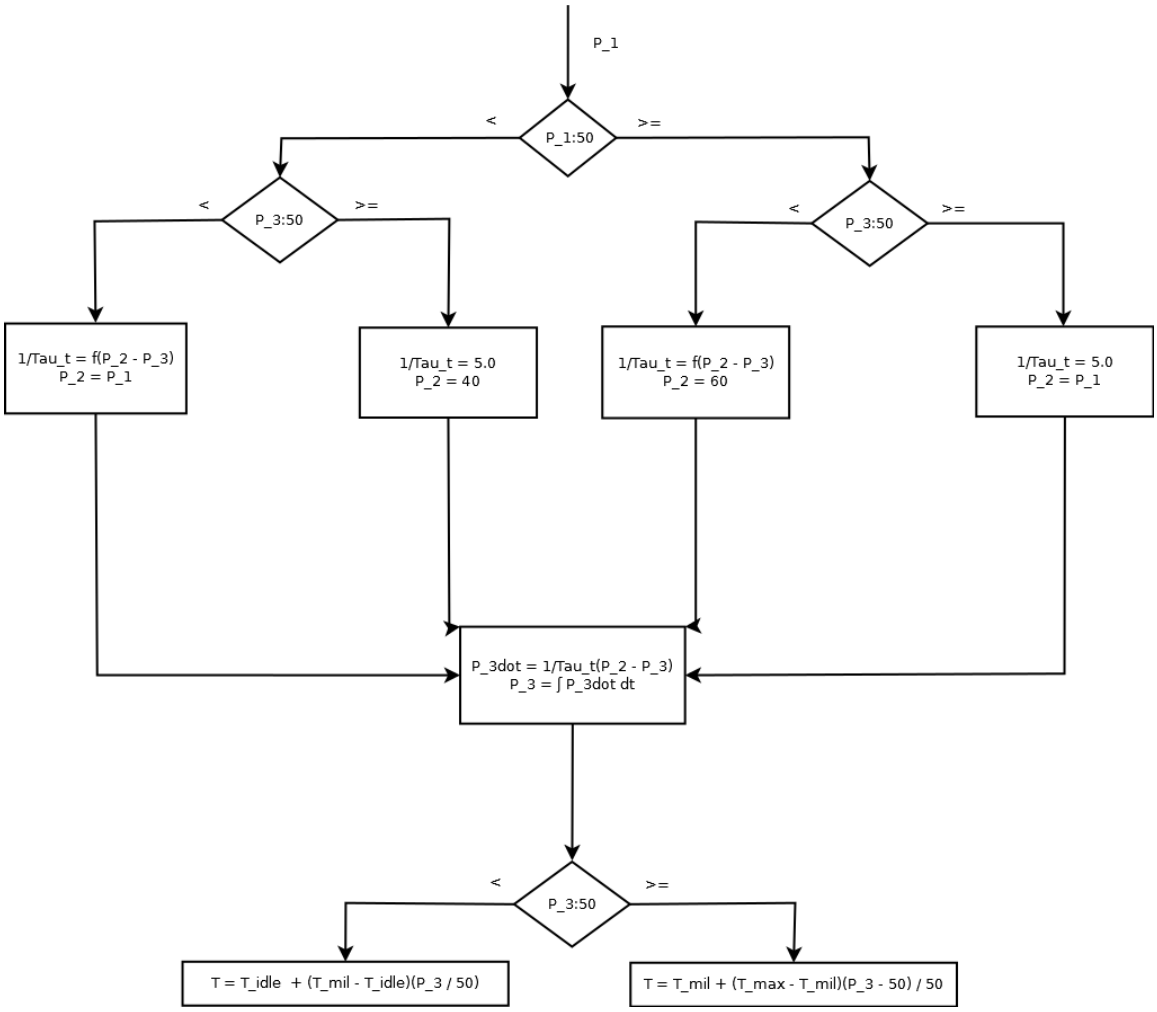

Figure A.1: Thrust dynamic model logic diagram [22]

B. Derivatives of aerodynamic coefficients

$$C_{l_p} = \frac{\partial C_l}{\partial \frac{pb}{2V}} \quad C_{l_r} = \frac{\partial C_l}{\partial \frac{rb}{2V}} \quad C_{l_\beta} = \frac{\partial C_\zeta}{\partial \zeta} \quad C_{\zeta_\beta} = \frac{\partial C_\zeta}{\partial \delta_a}$$

$$C_{l_{\delta_r}} = \frac{\partial C_l}{\partial \delta_r} \quad C_{m_q} = \frac{\partial C_m}{\partial \frac{q\bar{c}}{2V}} \quad C_{n_p} = \frac{\partial C_n}{\partial \frac{pb}{2V}} \quad C_{n_r} = \frac{\partial C_n}{\partial \frac{rb}{2V}}$$

$$C_{n_\beta} = \frac{\partial C_n}{\partial \beta} \quad C_{n_\beta,dyn} = C_{n_\beta} - \frac{I_Z}{I_X} C_{l_\beta} \sin\alpha \quad C_{n_{\delta_a}} = \frac{\partial C_n}{\partial \delta_a} \quad C_{n_{\delta_r}} = \frac{\partial C_n}{\partial \delta_r}$$

$$C_{X_q} = \frac{\partial C_X}{\partial \frac{q\bar{c}}{2V}} \quad C_{Z_q} = \frac{\partial C_Z}{\partial \frac{q\bar{c}}{2V}} \quad C_{Y_p} = \frac{\partial C_Y}{\partial \frac{pb}{2V}} \quad C_{Y_r} = \frac{\partial C_Y}{\partial \frac{rb}{2V}}$$

C. Content of the DVD

An enclosed DVD disc contains following:

- this document in `pdf` format
- `latex` source files of this document
- *Matlab* and *Simulink* files which contain the implementation of the work
- `README` file with detailed description of the DVD content
- Manual for *Matlab* and *Simulink* files